Langmuir

LETTER

pubs.acs.org/Langmuir

Reusable Antifouling Viscoelastic Adhesive with an Elastic Skin

Sandip Patil, Abhinav Malasi, Abhijit Majumder, Animangsu Ghatak, and Ashutosh Sharma*

Department of Chemical Engineering and DST Unit on Nanosciences, Indian Institute of Technology, Kanpur-208016, U.P., India

ABSTRACT: Although the viscoelasticity or tackiness of a pressure-sensitive adhesive gives it strength owing to energy dissipation during peeling, it also renders it nonreusable because of structural changes such as the formation of fibrils, cohesive failure, and fouling. However, an elastic layer has good structural integrity and cohesive strength but low adhesive energy. We demonstrate an effective composite adhesive in which a soft viscoelastic bulk layer is imbedded in a largely elastic thin skin layer. The composite layer is able to meet the conflicting demands of the high peel strength comparable to the viscoelastic core and the structural integrity, reusability, and antifouling properties of the elastic skin. Our model adhesive is made of poly(dimethylsiloxane), where its core and skin are created by varying the cross-linking percentage from 2 to 10%.

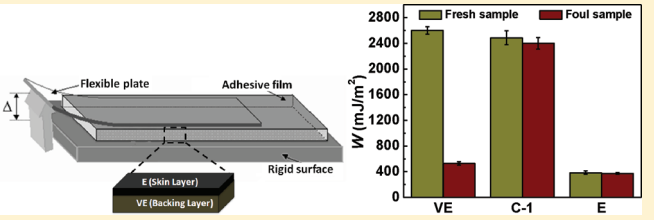

INTRODUCTION

Both elasticity and viscoelasticity play important roles in the performance of soft pressure-sensitive adhesives (PSAs). An effective pressure-sensitive adhesive during bonding should flow and deform easily to contact the surface conformally.[1,2] During debonding, however, it should have sufficient cohesive strength to resist a bulk failure and large energy dissipation for the greater work of adhesion.[3−6] The debonding is often accompanied by morphological changes such as fingering, cavitation, and fibrillation[7−12] both in elastic as well as in viscoelastic adhesives, which are processes that dissipate energy and form the major contributions to the total fracture toughness of an adhesive tape.[13] Although the fracture toughness thus achieved by a viscoelastic layer may be satisfactory,[14,15] the viscoelasticity or tackiness also prevents reusability. The surface changes that occur during detachment such as the generation of a rough surface, cohesive failure, and particulate contamination are often permanent and unavoidable in the case of soft viscoelastic surfaces.[16] Rheological properties[4,6,17,18] thus play important roles in PSAs, and hence different ways of controlling rheological properties are utilized in both natural and commercial adhesives. Whereas in commercially available adhesives the rheological properties are mostly uniform and isotropic and controlled by playing with chemical structures and additives, in natural adhesive pads such as those found in geckoes and insects, pad stiffness is controlled by complex hierarchical composite structures.[19−21] Recently, in bioinspired adhesives, some others factors that have been shown to influence adhesion are crack initiation and arrest,[22,23] buried microcapillaries, and micropillars.[24,25]

Here, we propose the simplest architecture for a dual-functionality composite layer PSA where the conflicting requirements of high peel strength are met with those of reusability by the minimization of cohesive failure, morphological changes, and fouling. The composite consists of a softer, more dissipative viscoelastic core layer capped by a much thinner but relatively stiffer elastic skin layer of the same material. The results for this composite architecture are explored for the layers made of polydimethylsiloxane (PDMS) elastomer, which can be cross-linked to different extents to readily vary its viscoelasticity. The adhesion and fouling of the composite layers are compared and contrasted with single viscoelastic and elastic adhesive layers.

MATERIALS AND METHODS

Adhesives used in the experiments were fabricated by using PDMS (Sylgard 184, Dow Corning) that contains an elastomer and a cross-linking agent. The elastomer and cross-linking agents were mixed in a ratio of 50:1 w/w (or 2% cross-linked PDMS) and 10:1 w/w (or 10% cross-linked PDMS) separately in a 25 mL clean glass beaker and degassed under vacuum by using a desiccator in order to have air-bubble-free PDMS solutions.[26] First, a 2% cross-linked PDMS solution was spin coated at different speeds in order to obtain different thicknesses (40 to 520 μm) on clean glass substrates and cured at 85 °C for 48 h. After the 2% cross-linked PDMS (backing) layer was coating and cured, a 10% cross-linked PDMS liquid (skin layer) was used to coat cured 2% cross-linked PDMS layers to thicknesses of 2, 15, 30, and 100 μm and then was fully cured. This protocol has been used earlier[11] to prepare smooth bilayers of 2 and 10% cross-linked PDMS in which no gross intermixing or distortion of the two PDMS interfaces is observed.

RESULTS AND DISCUSSION

The adhesive strength of the single and composite layers was estimated by using a displacement controlled peel test.[22,24] Figure 1 shows a schematic of the peel setup, where a self-assembled monolayer of an octadecyltrichlorosilane (OTS)-coated flexible glass coverslip was brought into complete contact with the adhesive surface and lifted vertically from its hanging edge at a constant peeling speed of 100 μm/s by using a linear stage controlled by a micromanipulator. The flexibility of the coverslip was chosen in such a way that it undergoes slight bending during peeling, and it allowed the measurement of the adhesion strength. Here we

Received: October 2, 2011
Revised: November 30, 2011
Published: December 27, 2011

   dx.doi.org/10.1021/la203871c | *Langmuir* 2012, 28, 42–46

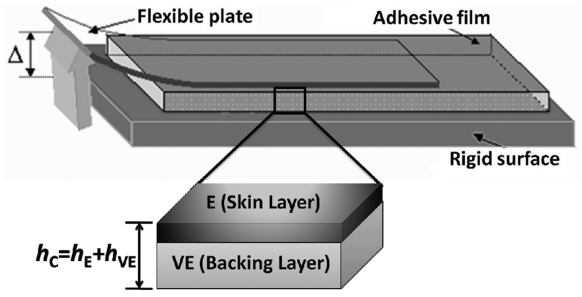

Figure 1. Schematic of the peel setup. A flexible glass coverslip of rigidity $D = 0.02$ N m was attached to the adhesive film. Here h_C, h_E, and h_{VE} represent the thicknesses of the composite and the elastic and viscoleastic layers, respectively, and Δ represents the displacement of the coverslip.

report the adhesion strength of the interface as the energy required to separate the two surfaces, including the viscoelastic energy dissipation in the film and the bending energy of the thin glass plate (minor component).

The variation of the force required for peeling, F, was measured and recorded by a strain gauge force sensor. The adhesion strength for the crack propagation was evaluated by integrating the area under the curve for the peeling force, F, versus the displacement of the cover plate, Δ, starting from the maximum force (i.e., crack-initiation point to the point of detachment). The total adhesion strength is divided by the contact area (300 mm^2) to obtain the adhesion strength per unit area reported here. The force−displacement ($F-\Delta$) curves for a single viscoelastic layer, a single elastic layer, and the composite layers are shown in Figure 2. For the composite layer, the thickness of the viscoelastic backing layer was kept constant at h_{VE} = 420 μm, and four different thicknesses for the elastic skin layer were used (h_E = 2, 15, 30, and 100 μm).

The $F-\Delta$ curves for all of these different adhesive combinations are characterized by a crack initiation regime where the peak force is attained rapidly followed by a more gradual decay in the crack-propagation regime. This behavior is similar to that observed in a typical peel experiment.[22,24] An elastic layer (E in Figure 2) snaps out of contact catastrophically owing to a lack of viscous dissipation, whereas slow crack propagation restricted by the viscous dissipation in the core occurs for the composite layers (C-1 to C-4), as also in a single viscoelastic layer (VE). The crack initiation force, as indicated by the peak in an $F-\Delta$ curve, is much higher in the viscoleastic and composite layers than in the elastic layer because of the higher compliance. Compliance is the ease of deformation of the layer on application of an external load. As a first approximation, the compliance of the layer can be defined as h/shear modulus. These two factors, namely, a higher compliance and viscous dissipation, contribute to the higher adhesive strength of the viscoelastic layer compared to that of the elastic layer. The crack propagation dynamics in elastic and viscoelastic adhesives is governed by the competition between the energy release rate, G_c, and the material's resistance toward bulk deformation. For the linear elastic adhesive, the bulk deformation is essentially controlled by the elastic modulus of the material, E, and thus the displacement of the adhesive before final detachment is governed by the ratio of these two parameters: G_c/E. When E is large (stiffer material) or G_c/E is small, the adhesive deforms less and comes off of the contactor quickly, and thus the crack propagates catastrophically. For an elastic thin film, this

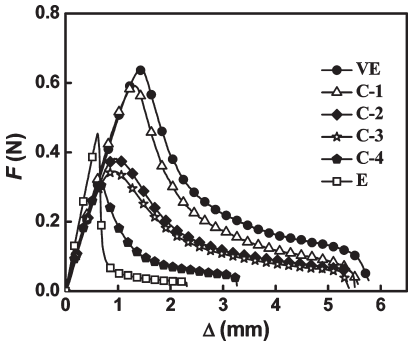

Figure 2. Force−displacement ($F-\Delta$) curves obtained from the peel test. C-1 to C-4 represent composite layers with skin layer thicknesses of h_E = 2, 15, 30, and 100 μm, respectively, and a backing layer thickness of 420 μm. The peel test comparison is also done for a single adhesive layer of elastic PDMS (E) and a viscoelastic PDMS (VE) with a thickness of 420 μm each.

competition between interfacial interactions to elastic deformation leads to reversible instability morphologies.[10−12] However, for a viscoelastic adhesive, the relationship is far more complex that in the situation where G_c itself is a function of the crack propagation velocity. Although G_c/E still can be used as the predictor of the crack propagation rate, here G_c is much more difficult to quantify. To address this question, Deplace et al.[27] proposed a simpler viscoelastic measure of the crack propagation, $\tan\delta/G'$, assuming a relatively weak adhesion due to the van der Waals force alone. Although the assumption is crude, this parameter can at least qualitatively explain the crack propagation behavior for an elastic and a viscoelastic adhesive.

Figure 3 show the rheological response for elastic and viscoelastic PDMS used in this study. From Figure 3a we estimate the storage, $G'(f)$, and loss, $G''(f)$, moduli for used PDMS systems. For elastic (10% cross-linked) PDMS, the storage modulus is higher than the loss modulus, indicating a nearly frequency-independent elastic solid. For viscoelastic (2% cross-linked) PDMS, the storage and loss moduli become comparable at a moderate frequency. There is nearly 1 order of magnitude difference in the storage moduli and 2 orders of magnitude difference in the loss moduli of the two PDMS layers. The ratio G''/G', which is called the loss tangent, $\tan\delta$, is high ($\gg 1$) for materials that are viscoelastic liquidlike but low ($\ll 1$) for materials that are solidlike. Furthermore, $\tan\delta/G'$ as shown in Figure 3b is indicative of the viscous dissipation, which also controls the crack propagation speed.[27] The viscous dissipation is clearly controlled by the 2% cross-linked PDMS layer.

The higher value of $\tan\delta/G'$ for the viscoelastic layer corresponds to a higher displacement of the adhesive layer before failure, which is manifested by higher peaks and slower crack propagation compared to those of the elastic layer. The composite layers, C-1 to C-4 (h_E = 2, 15, 30, and 100 μm), show intermediate behavior in Figure 2 as expected. However, the skin-layer thickness has a prominent effect. As the skin layer thickness increases, the composite performance becomes increasingly similar to that of the elastic film. Although the adhesive behavior of composite C-1 with the thinnest elastic skin is almost identical to that of the single viscoelastic film with an unshielded surface, composite C-4 closely approaches a single elastic layer. The decay in force for composite films parallels the viscoelastic case signifying the control of detachment by dissipation in the buried

dx.doi.org/10.1021/la203871c |*Langmuir* 2012, 28, 42–46

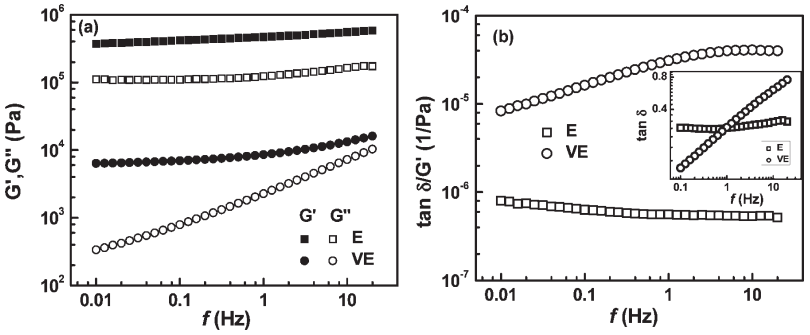

Figure 3. (a) Storage, G', and loss, G'', moduli and (b) tan δ/G' for the elastic (E) and viscoelastic (VE) PDMS used in this study. The inset shows the behavior of tan δ as function of frequency .

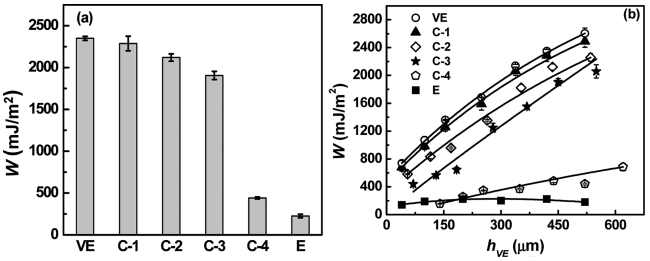

Figure 4. Adhesion strength of viscoelastic (VE), composite (C-1 to C-4), and elastic (E) layers. (a) Composite layers C-1 to C-4 have elastic skin layer thicknesses of 2, 15, 30, and 100 μm, respectively. The thickness of the single layers and the core layer is 420 μm. (b) Variation of adhesion strength with layer thickness. For composite layers C-1 to C-4, the skin thicknesses are kept constant at 2, 15, 30, and 100 μm, respectively, and the thickness of the viscoelastic core layer is varied. The error bars shown in parts a and b are calculated from the standard deviation of six experimental runs on three different samples, and lines joining the data points are guides for the eye rather than a fit.

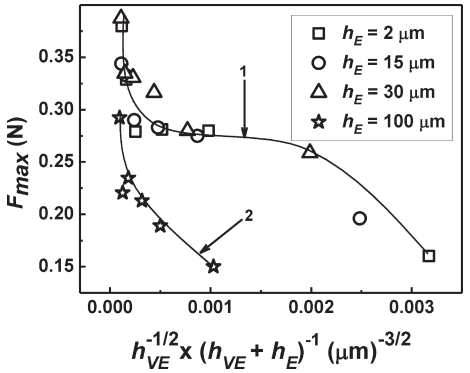

Figure 5. Variation of the maximum pull-off force, F_{max}, as a function of $h_{VE}{}^{-0.5}(h_{VE} + h_E)^{-1}$. Curves 1 and 2 represent two different regimes of F_{max} dependency as a function of thickness. Curve 1 shows all of the experimental values of F_{max} for skin layers of 2, 15, and 30 μm for different backing layers of 45, 100, 154, 249, 338, and 420 μm falling on the same line as function $h_{VE}{}^{-0.5}(h_{VE} + h_E)^{-1}$. However, curve 2 shows a slight variation in F_{max} as a function of $h_{VE}{}^{-0.5}(h_{VE} + h_E)^{-1}$.

viscoelastic layer, notwithstanding the presence of the elastic skin. The higher peak forces and their slower decay are also reflected in the higher adhesion strength or the work of adhesion as shown in Figure 4. The estimated adhesion strengths for a single elastic layer and viscoelastic layers are W = 180 and 2350 mJ/m^2, respectively (both for 420-μm-thick films). As noted previously, the adhesion strength shown is only for the crack-propagation part of the $F-\Delta$ curve. However, as is clear from Figure 2, the crack-initiation strength (area from zero to the maximum force) is also significantly higher for the composite adhesive.

The adhesion strength of the composite layers shows intermediate behavior depending on its skin thickness. For a very thin elastic skin layer (h_E = 2 μm), the adhesion strength is nearly identical to that of a corresponding single viscoelastic layer. A greater penetration of the stress field in the viscoelastic core during peeling allows a greater arresting effect for the crack owing to greater viscous dissipation. A thick (>100 μm) elastic skin, however, completely shields the viscoelastic core from the stresses, and the adhesion strength falls to its low value for a single elastic layer.

We varied also the core layer thickness from 40 to 520 μm while keeping the skin layer thickness constant. The results for the composites are compared to the single elastic and viscoelastic layers in Figure 4b. The plots reveal that for a single viscoelastic (elastic) layer the adhesion strength shows a strong (weak) thickness dependence. A similar observation was explained by Gent et al.[28] and Kinloch[29] by considering the change in the elastic compliance and deformation properties with thickness. For the bilayers, C-1 to C-3 follow the viscoelastic curve in parallel whereas the trend for C-4 is almost the same as for a single elastic layer. This observation implies that the shielding effect of the elastic top layer is predominantly dependent on the top layer thickness and not on the ratio of the two layers. In this study, we have kept the glass coverslip thickness and flexural rigidity constant at 120 μm and 0.02 N m, respectively, for easy comparison.

The above observation is rationalized by considering the load required to lift a thin, flexible plate off a thin layer of elastic adhesive.[22] For a crack length, a, the lifting load, F, applied to a plate was obtained as a function of the lift-off height, Δ, the flexural rigidity of the plate, D, and the elastic modulus of the film, G',[22]

$$F = \frac{\Delta D k^3}{f(ak)}$$

where

$$f(ak) = \frac{6 + 12(ak) + 9(ak)^2 + 2(ak)^3}{6}$$

Here $k^{-1} = ((Dh^3)/(12G'_{eff}))^{1/6}$ has a dimension of length and defines the distance from the contact line within which the stresses

dx.doi.org/10.1021/la203871c |Langmuir 2012, 28, 42–46

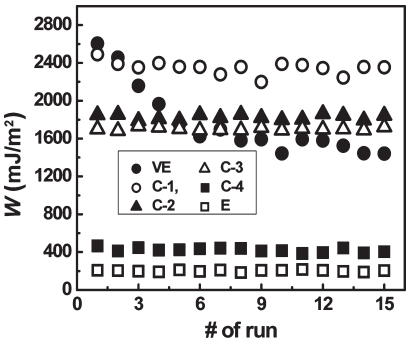

Figure 6. Variation of the adhesion strength after a number of adhesion−debonding cycles for the viscoelastic (VE), elastic (E), and composite layers (C) but without any cohesive failure or fouling. The thickness of each viscoelastic/elastic single layer and the composite backing layer is 420 μm, and the skin thicknesses of composite layers C-1 to C-4 are 2, 15, 30, and 100 μm, respectively.

remain concentrated. For an elastic bilayer (composite), its effective deformability in the limit $h_{VE} \gg h_E$ can be approximately expressed as[22]

$$\frac{h}{G'_{eff}} = \frac{h}{G'_E} + \frac{h_{VE}}{G'_{VE}} h = h_{VE} + h_E$$

However, because $G_E' \gg G_{VE}'$, the above relation simplifies to

$$\frac{h}{G'_{eff}} = \frac{h_{VE}}{G'_{VE}}$$

Using above relation, the expression for F can be simplified to

$$F = \frac{\Delta D}{f(ak)}\left(\frac{12G'_{eff}}{Dh^3}\right)^{1/2} = \frac{\Delta D}{f(ak)}\left(\frac{12G'_{eff}}{Dh}\right)^{1/2}\frac{1}{h}$$
$$= \frac{\Delta D}{f(ak)}\left(\frac{12G'_{VE}}{Dh_b}\right)^{1/2}\frac{1}{h} = \frac{\Delta(12DG'_{VE})^{1/2}}{f(ak)}\frac{1}{{h_{VE}}^{1/2}}\frac{1}{h}$$

Notice that $f(ak)$ is not independent of h, but we can assume that for different parameters of the composite layer its value will not be very different. Therefore, we plot the maximum detachment force, F_{max}, obtained from the peel test of composite adhesives of four different elastic skin layer thicknesses (2, 15, 30, and 100 μm) as a function of ${h_{VE}}^{-1/2}h^{-1}$ in Figure 5. The data show that the elastic skin layer thickness significantly affects the lifting load F_{max}; the data are slightly scattered for skin layers of 2 to 30 μm even though the F_{max} values of all of the experimental runs can be successfully predicted by a single line (curve 1) once they are plotted as a function of ${h_{VE}}^{-0.5}(h_{VE} + h_E)^{-1}$. However, this master curve is not a straight line possibly because of the functional dependence of $f(ak)$ on h, which we have neglected here. Furthermore, the data for the 100 μm skin layer thickness does not fall on this master curve because the assumption of $h_{VE} \gg h_E$ does not remain valid. Although the simple extension of the analysis of an elastic system captures the general behavior of this bilayer system, a more detailed analysis is necessary in order to account for the true viscoelastic character of the system.

Nevertheless, the above results show the feasibility of achieving a nontacky, nonstick surface of a sticky composite that approaches the peel strength of a viscoelastic layer by the proper selection of the thicknesses and rheological properties. The next important objective is to study the reusability and

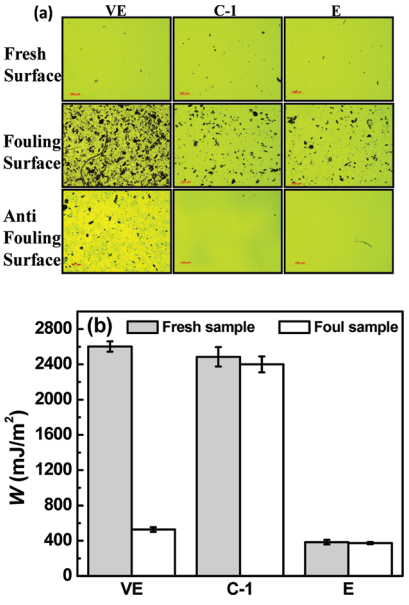

Figure 7. (a) Optical micrographs of surfaces after a fouling test for the viscoelastic (VE), composite (C-1), and elastic (E) surfaces. The thickness of the viscoelastic/elastic single layer and the backing layer is 420 μm, and the skin thickness for composite C-1 is 2 μm. (First row) Fresh adhesive surfaces, (second row) the dirt attached to adhesive surfaces after an air spray, and (third row) adhesive surfaces after the removal of dust by an adhesive tape to assess the ease of surface cleaning. (b) Adhesion strength on fouled samples after cleansing with an air jet and adhesive tape. The filled bars and the empty bars show the adhesive energies of the fresh and fouled samples. Thickness of viscoelastic/elastic single layer and backing layer are 420 μm and for the composite layer C-1, skin thickness is 2 μm.

antifouling characteristics of these composite adhesives. In this context, the peel test was repeated 15 times on the same area of the adhesive film to determine its reusability characteristics. However, care was taken to avoid fouling the peeled surfaces by conducting these tests in a class 1000 clean room. As shown later, fouling is another real-life complexity that can severally limit the reusability of a tacky surface but not an elastic surface. Figure 6 depicts the reusability of various adhesives. Interestingly, only a viscoelastic layer shows a drastic loss of adhesive strength with repeated use but eventually stabilizes to a much lower adhesive strength after about six cycles of adhesion and debonding. Decreasing adhesion strength could be owing to the extraction of chains from adhesive surface onto the glass plate repetitively[30,31] and possibly also to the roughening of the viscoelastic surface during peeling.[32] However, an elastic adhesive film and all of the composites with elastic skins show no change in their adhesive strengths after repeated use.

Furthermore, the fouling of a peeled adhesive surface by dirt and debris is another important factor that limits the reusability of an adhesive layer. Clearly, a nonsticky, nonfouling surface may also be preferable in many other applications such as in sensing and bioadhesives. Figure 7a provides a quick measure of the fouling characteristics of various adhesive surfaces. Row 1 in Figure 7a shows optical images of freshly prepared viscoelastic, composite, and elastic PDMS adhesive surfaces. Dirt particles (0.5 g) were then uniformly sprinkled on these surfaces by using a fine mesh, and the surfaces were cleaned by controlled air spraying. Row 2 in Figure 7 shows residual dirt after air spraying.

dx.doi.org/10.1021/la203871c |*Langmuir* 2012, 28, 42–46

The viscoelastic adhesive was left with more residual particles compared to the composite and elastic adhesives. We then cleaned the surfaces by applying commercial adhesive tape to and peeling it off of the dirty surfaces (Figure 7a, row 3). This procedure could clean the elastic surfaces fairly well but not the viscoelastic surface. To assess the influence of fouling on adhesion, the surfaces cleaned with the air jet and subsequently with the adhesive tape were subjected to the peel test. Figure 7b summarizes the results. Although there is no change in the adhesion of the composite and elastic layers, the adhesive strength of the viscoelastic film drops by about an order of magnitude owing to the residual debris.

OUTLOOK

We propose a simple architecture of an effective soft adhesive where a viscoelastic imbedded backing or core layer engenders the high strength of adhesion by its high compliance and viscous dissipation, whereas a thin elastic skin layer provides structural integrity, reusability, and nonfouling characteristics owing to its nonsticky nature. Such a multilayer adhesive is compatible with the roll-to-roll manufacturing requiring no special patterning tool, and its adhesive properties can be tuned by the viscoelasticity of the core and the thickness of the elastic skin and the viscoelastic backing layer. Thin-skinned composite layers approaching the adhesive strength of the imbedded viscoelastic layer are found to be reusable and nonfouling, the twin characteristics missing in a single viscoelastic layer.

AUTHOR INFORMATION

Corresponding Author

*E-mail: ashutos@iitk.ac.in. Telephone: +91-512-2597026. Fax: +91-512-2590104.

ACKNOWLEDGMENT

A.S. acknowledges the support of the DST through its grants to the Unit on Soft Nanofabrication and an IRHPA grant.

REFERENCES

(1) Greenwood, J.; Johnson, K. *The Mechanics of Adhesion*; Elsevier: Amsterdam, 1981.
(2) Creton, C.; Papon, E. *Mater. Sci.* **2003**, 419–423.
(3) Carelli, C.; Déplace, F.; Boissonnet, L.; Creton, C. *J. Adhes.* **2007**, *83*, 491–505.
(4) Creton, C.; Hooker, J.; Shull, K. R. *Langmuir* **2001**, *17*, 4948–4954.
(5) Shull, K. R.; Creton, C. *J. Polym. Sci., Part B: Polym. Phys.* **2004**, *42*, 4023–4043.
(6) Leger, L.; Creton, C. *Philos. Trans. R. Soc., A* **2008**, *366*, 1425–1442.
(7) Creton, C.; Fabre, P. *Adhes. Sci. Eng.* **2001**, *2*, 1–24.
(8) Nase, J.; Creton, C.; Ramos, O.; Sonnenberg, L.; Yamaguchi, T.; Lindner, A. *Soft Matter* **2010**, *6*, 2685–2691.
(9) Nase, J.; Lindner, A.; Creton, C. *Phys. Rev. Lett.* **2008**, *101*, 074503–4.
(10) Tomar, G.; Sharma, A.; Shenoy, V.; Biswas, G. *Phys. Rev. E* **2007**, *76*, 011607–8.
(11) Mukherjee, R.; Pangule, R.; Sharma, A.; Tomar, G. *Adv. Funct. Mater.* **2007**, *17*, 2356–2364.
(12) Ghatak, A.; Chaudhury, M. K.; Shenoy, V.; Sharma, A. *Phys. Rev. Lett.* **2000**, *85*, 4329–4332.
(13) Creton, C. *MRS Bull.* **2003**, *28*, 434–439.
(14) Passade, N.; Creton, C.; Gallot, Y. *Polymer* **2000**, *41*, 9249–9263.
(15) Wei, Y.; Hutchinson, J. W. *Int. J. Fract.* **1998**, *93*, 315–333.
(16) Chiche, A.; Creton, C. *Proceeding of the 27th Annual Adhesion Society Meeting*; Wilmington, NC, 2004; pp 296−298.
(17) Dahlquist, C. A. Pressure Sensitive Adhesives; In *Treatise on Adhesion and Adhesives*, 2nd ed.; M. Dekker:New York, 1969.
(18) Yarusso, D. J. *Effect of Rheology on PSA Performance*; Elsevier: Amsterdam, 2002.
(19) Arzt, E.; Gorb, S.; Spolenak, R. *Proc. Natl. Acad. Sci., U.S.A.* **2003**, *100*, 10603–10606.
(20) Gorb, S.; Gorb, E.; Kastner, V. *J. Exp. Biol.* **2001**, *204*, 1421–1431.
(21) Autumn, K.; Liang, Y. A.; Hsieh, S. T.; Zesch, W.; Chan, W. P.; Kenny, T. W.; Fearing, R.; Full, R. J. *Nature* **2000**, *405*, 681–865.
(22) Ghatak, A.; Mahadevan, L.; Chung, J. Y.; Chaudhury, M. K.; Shenoy, V. *Proc. R. Soc. London, Ser. A* **2004**, *460*, 2725–2735.
(23) Chung, J. Y.; Chaudhury, M. K. *J. R. Soc., Interface* **2005**, *2*, 55–61.
(24) Majumder, A.; Ghatak, A.; Sharma, A. *Science* **2007**, *318*, 258–261.
(25) Glassmaker, N. J.; Jagota, A.; Hui, C.-Y. *Acta Biomater.* **2005**, *1*, 367–375.
(26) Mukherjee, R.; Pangule, R. C.; Sharma, A.; Banerjee, I. *J. Chem. Phys.* **2007**, *127*, 064703–6.
(27) Deplace, F.; Carelli, C.; Mariot, S.; Retsos, H.; Chateauminois, A.; Ouzineb, K.; Creton, C. *J. Adhes.* **2009**, *85*, 18–54.
(28) Gent, A. N.; Hamed, G. R. *Polym. Eng. Sci.* **1977**, *17*, 462–466.
(29) Kinloch, A. J. *Adhesion and Adhesives: Science and Technology*; Chapman and Hall: London, 1987.
(30) Briggs, G. A. D.; Briscoe, B. J. *J. Phys. D: Appl. Phys.* **1977**, *10*, 2453–2466.
(31) Creton, C.; Leibler, L. *J. Polym. Sci., Part B: Polym. Phys.* **1996**, *34*, 545–554.
(32) Kumar, J.; Ananthakrishna, G. *Phys. Rev. E* **2010**, *82*, 016211–13.